Combustion of Polymethylmethacrylate in a Solid Fuel Ramjet

P. A. O. G. Korting*
Prins Maurits Laboratory TNO, Rijswijk, the Netherlands
C. W. M. van der Geld†
Eindhoven University of Technology, Eindhoven, the Netherlands
T. Wijchers‡
Delft University of Technology, Delft, the Netherlands
and
H. F. R. Schöyer§
ESA/ESTEC, Noordiwijk, the Netherlands

The combustion behavior of polymethylmethacrylate (PMMA) in a solid fuel ramjet (SFRJ) was investigated using a connected pipe test facility. The study was oriented towards understanding the most important phenomena related to the combustion in an SFRJ. Regression rates have been determined, and spectroscopy has shown the occurrence of OH, C_2, and CH. Combustion pressure was shown to affect soot formation. No grain length effect on regression rate could be detected, whereas oxygen content in the air and inlet air temperature are important. Temperatures in the center of the bore are about 900 K, while temperatures in the recirculation zone approximate 1400 K. The highest temperatures were found in the near-wall region downstream of the recirculation zone. The combustion efficiency varied between 70% and 90%, and may be increased by increasing the fuel grain length and/or the oxygen content.

Nomenclature

cc = correlation coefficient
d_{p0} = initial port diameter
G = average total mass flux
h = stepheight
h_0 = initial stepheight
$h_{v_{\text{eff}}}$ = effective heat of gasification
L = length
L_g = grainlength
L_r = recirculation zone length
m_{air} = air mass flow rate
p = pressure
p_c = mean pressure in aft mixing chamber
q_c, q_c' = convective heat transfer
q_r = radiative heat transfer
q_w = heat transfer to fuel surface
r = regression rate
T = temperature
T_r = radiation temperature
T_{wall} = wall temperature
ϵ_g = emission coefficient of the gas mixture
ϵ_w = wall absorption coefficient
ρ_F = fuel density
σ = Stephan-Boltzman constant

Introduction

FIGURE 1 schematically depicts the combustion chamber of a solid fuel ramjet (SFRJ). Highly turbulent air enters from the left and establishes a recirculation zone downstream of a rearward facing step. After reattachment of the flow directly behind the recirculation region, a turbulent boundary layer starts to build up. The fuel pyrolysis gases mix and react with the air. The combustion products then pass through an aft mixing chamber and are exhausted through a nozzle.

The present work concerns test runs with polymethylmethacrylate (PMMA) and ambient air, oxygen enriched air, and air at elevated temperatures in such an SFRJ. Emphasis was laid on determining the regression rate and combustion efficiency. Temperature measurements in the combustion chamber were obtained from radiation measurements and by means of spectroscopic equipment. The latter also allowed for species identification.

Experimental Apparatus

Test Facility

The connected pipe test facility[1] used in these experiments is operated and controlled via a computer. "Air" at precisely controlled temperatures was produced via a vitiator in which methane is burned with oxygen enriched air. The oxygen content of the exhaust gases was kept the same as that of air. An especially developed Sonic Control and Measuring Choke guaranteed constant (total) mass flow rates and allowed for accurate mass flow rate measurements.

Combustion Chamber

The combustion chamber consisted of an injection chamber, a cast fuel grain with a nominal length of 300 mm, and an aft mixing chamber (see Fig. 2); also fuel grains with lengths of 500, 700, and 900 mm were used. Aft mixing chamber lengths were 170 and 270 mm. The nominal inner grain diameter before burning was 40 mm, the outer diameter was 70 mm. Flame stabilization was achieved by an orifice-type rearward-facing step.

Optical Instrumentation

Chordal-beam-averaged temperatures, axis-averaged temperatures, and the kind of species present in the motor were derived from spectra (see Fig. 3). Two different light paths were used in the axial direction via mirrors M1 and M2 and in the radial direction via mirror M2. In both cases, the light was collimated by lense L1, passed through a hole in the wall of the test room and then focused by lens L2 on the entrance slit S of

Received June 15, 1987; revision received May 10, 1989.

*Head of Rocket Propulsion Section. Member AIAA.
†Senior Faculty Member, Faculty of Mechanical Engineering.
‡Senior Faculty Member, Faculty of Aerospace Engineering.
§Head of ESTEC Chemical Propulsion Section, Consultant Prins Maurits Laboratory TNO. Member AIAA.

a 1-m grating spectrograph Sp. A multichannel detector D with an intensifier was read after each exposure by controller Ct. A computer Cp processed the recorded spectra. The efficiency of the optical train (length of 10 m) was about 45%. More details have been given by Wijchers[2] and Elands and Wijchers.[3]

Ultrasonic Instrumentation

For some tests, the local instantaneous regression rate was measured by means of an ultrasonic pulse echo technique.[4] Emitted pulses (2.25 MHz) were generated by an ultrasonoscope and reflected by the regressing fuel surface during combustion. The time lapse between the emitted and the received sound pulse was converted by an electronic system into a suitable output voltage. The effects of a temperature profile in the fuel were considered to accurately deduce the regression rate from the measured time lapse.

Results

General Combustion Behavior

A typical pressure history for cold inlet air is shown in Fig. 4. The initial pressure peak was due to ignition by an H_2/O_2 flame. This history shows that about 15 s were required to obtain full flame development. For heated air, this time was greatly reduced. High-speed cine films showed that the combustion process started in the recirculation zone and proceeded gradually downstream in the fuel grain. At pressures below 0.5 MPa, a transparent blue flame was observed indicating hardly any soot formation. At higher pressures the flame became yellow because of soot production; the optical density increased with increasing pressure.

Apart from the recirculation zone, the internal surface profile of the grain remained almost parallel to the center line (see Fig. 5), indicating an almost homogeneous regression rate. The maximum erosion was found at a distance of 8.5 to 9.5 stepheights from the entrance. This corresponds to the location of the reattachment point as calculated by Vos.[5] This reattachment point acts as a kind of stagnation point, where convective heat transfer, hence regression rate, are expected to attain their maximum value.

Light emission measurements not only showed a gradual increase in total light emission during burning but also a strongly oscillatory behavior; see Fig. 6. An analysis showed the frequencies to be between 70 and 100 Hz. These frequencies corresponded to a regular shedding of large-scale vortices

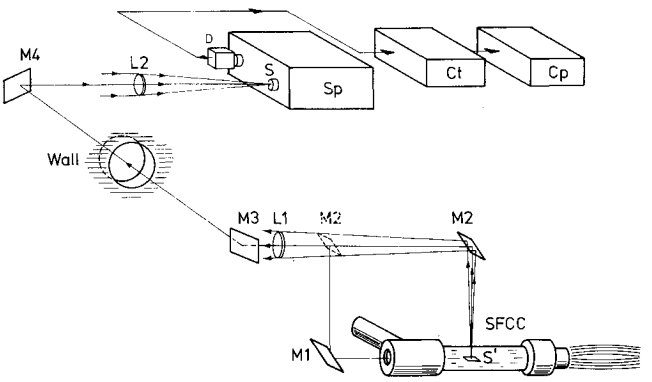

Fig. 3 Schematic diagram of spectrograph system (Sp: Jobin Yvon 1000S, 600 and 2400 1/mm; D: SI IRJ 1024, intensified diode array, 1024 channels on 25 mm).

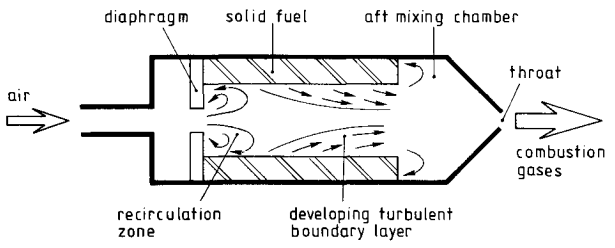

Fig. 1 Schematic of a solid fuel ramjet combustion chamber.

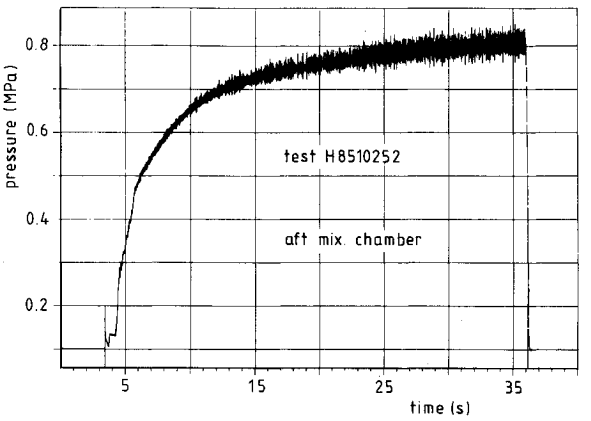

Fig. 4 Typical pressure history (PMMA/ambient air).

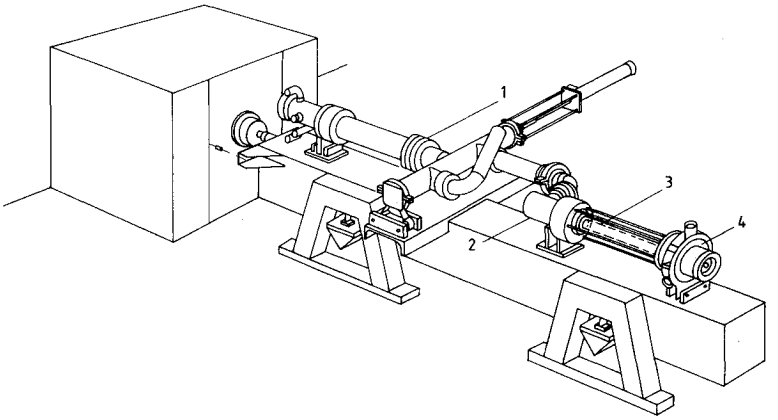

Fig. 2 Connected pipe facility: 1) Vitiator, 2) injection chamber, 3) solid fuel combustion chamber, 4) aft mixing chamber.

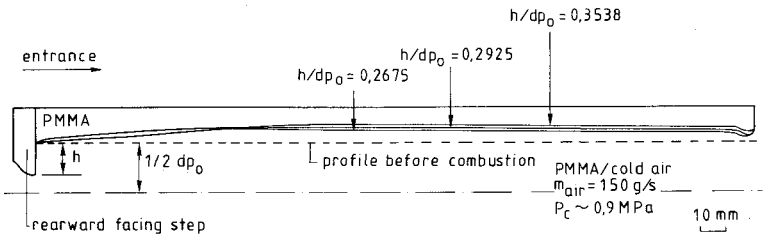

Fig. 5 Grain inner surface profiles after combustion, effect of step-height.

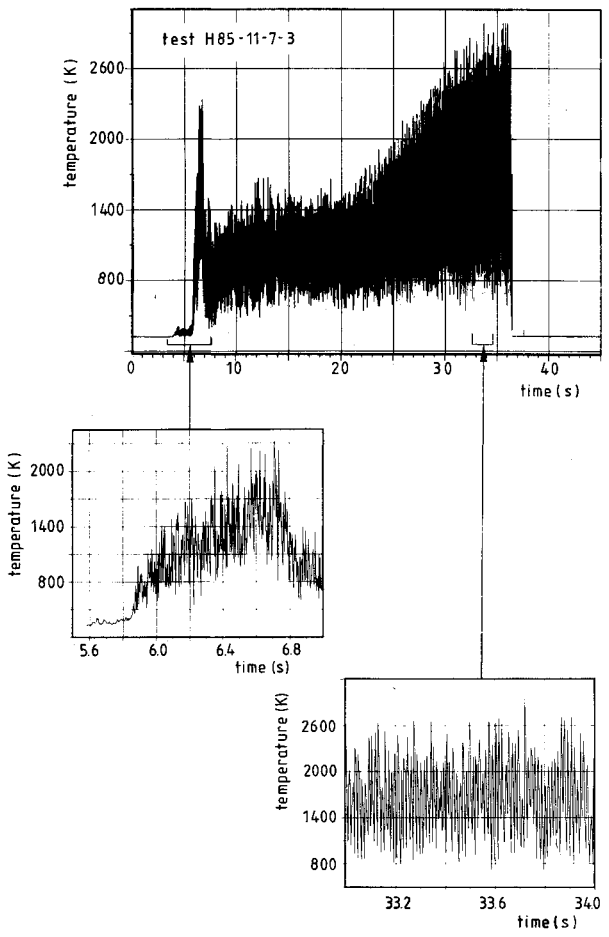

Fig. 6 Radiative temperature history measured by the radiation detector (PMMA/ambient air), chamber pressure 0.9 MPa.

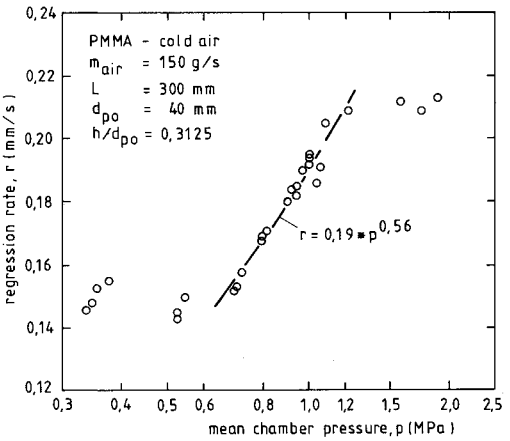

Fig. 7 Effect of pressure on regression rate due to soot formation.

directly downstream of the rearward-facing step, as was revealed by high-speed cine films. This shedding was governed by the acoustic field in the injection chamber and combustor. The frequency followed from the geometry.[6]

Chamber Pressure and Mass Flux Effects on Regression

Figure 7 shows that the regression rate vs pressure follows an S curve. Below 0.65 MPa little pressure sensitivity is noticed and hardly any soot is observed, suggesting radiative heat transfer is virtually absent. At higher pressures, where soot production becomes significant, the regression rate increases with chamber pressure according to

$$r = 0.19\,p^{0.56} \qquad (cc = 0.975,\ 0.65\ \text{MPa} \le p < 1.3\ \text{MPa}) \quad (1)$$

This result is in reasonable agreement with the observation of Mady et al.[7] Since soot appears above 0.65 MPa, it can be shown that the observed pressure effect can be attributed to radiative heat transfer to the surface. The net heat transfer to the surface

$$q_w = \rho_F h_{v_{\text{eff}}} r \quad (2)$$

is the sum of two contributions:

$$q_w = q_r + q_c' \quad (3)$$

where the radiation part follows from

$$q_r = \epsilon_w \epsilon_g \sigma (T_r^4 - T_{\text{wall}}^4) \quad (4)$$

and the convection part following Muzzy[8] is

$$q_c' = q_c e^{-q_r/q_c} \quad (5)$$

Equation (5) accounts for the reduction in heat transfer due to injection of pyrolysis gases (the blocking effect). Here q_c denotes the convective heat transfer if no radiation would be present.

Over the entire pressure region, spectroscopic measurements yielded T_r values of about 1800 K, and T_{wall} was estimated to be about 800 K. The latter temperature is higher than generally assumed; however, it is consistent with other measurements obtained in this laboratory. The wavelength averaged absorption coefficient of PMMA[9] is estimated to be 0.5, which yields an absorbed radiant heat flux of 0.29 MW/m^2 if the emission coefficient of the gas mixture is unity. For PMMA, $\rho_F \approx 1180$ kg/m^3 and $h_{v_{\text{eff}}} \approx 1.3$ MJ/kg. At pressures where the little soot is produced, r was measured to be about 0.15 mm/s (see Fig. 7). However, at pressures where the flame is definitely sooting, the ratio q_w/q_c now attains values between 1 and 1.5, as is easily seen from Eqs. (3-5). Note that the experimental value of r is increased by a factor of 1.4 if pressure is increased from 0.65 MPa up to 1.27 MPa and that r is proportional to q_w. Above 1.2 MPa there is so much soot in

the flow that the flame effectively acts as a blackbody radiator, and maximum radiative heat transfer is achieved. With increasing pressures, the regression rate therefore remains at the same level. The following conclusions are drawn:

1) Radiative heat transfer cannot be neglected when soot is present (see Ref. 10).

2) Radiation causes an increase of regression rate with increasing chamber pressure.

3) The maximum amount of radiative heat transfer is limited to blackbody radiation, independent of the mass flux. The convective heat transfer, however, increases with increasing mass fluxes. It is therefore expected that the observed pressure dependency diminishes with increasing mass fluxes.

Figure 8 shows that the regression rate is more dependent on convection at low pressures than at high pressures. This is in accordance with the previous observation.

Oxygen Content and Inlet Air Temperature Effect on Regression

The regression rate increases with oxygen content (see Fig. 9). Spectroscopic measurements show an increase in flame temperature with oxygen content, which implies an increase in convective heat transfer to the wall. A strong increase in regression rate at elevated inlet air temperatures was also observed (see Fig. 10). In the low-pressure region, the regression rate is about proportional to $T^{2/3}$. The authors are not aware of semiempirical correlations that could predict such a strong temperature dependency. However, sophisticated computer models for similar flows[11] indeed suggest this strong temperature dependency. With increasing pressures, at least up to 1.15 MPa, a decrease in the temperature exponent is observed. This result might be explained by the occurrence of radiation, which becomes significant above 0.6 MPa.

Stepheight and Grain Length Effect on Regression

An increase in stepheight increases the regression rate (see Fig. 11). This increase appears to be almost constant along the fuel grain downstream of the point of reattachment (see Fig. 5). Figure 12 shows only a weak relation between the regression rate and the grain length, in agreement with the homogeneous burning downstream of the reattachment point (see Fig. 5). A similar result has been found by Zvuloni et al.[12]

Since convective heat transfer diminishes as a boundary layer grows, the observed homogeneous burning can only be understood by an increase of radiative heat transfer due to increased soot production downstream along the fuel grain. The latter is confirmed by our observations, and by the calculations of Metochianokis and Netzer.[10]

Local Instantaneous Regression Rate

The local instantaneous regression rate was measured with an ultrasonic pulse echo sensor, located at distances of 110, 150, and 200 mm from the inlet. Typical results are shown in Fig. 13. Due to the high temperature H_2/O_2 ignition flame, the initial regression rate is relatively high during the first 5 s. The presence of the H_2/O_2 flame during this time is confirmed by the spectroscopic observation of a high OH concentration.

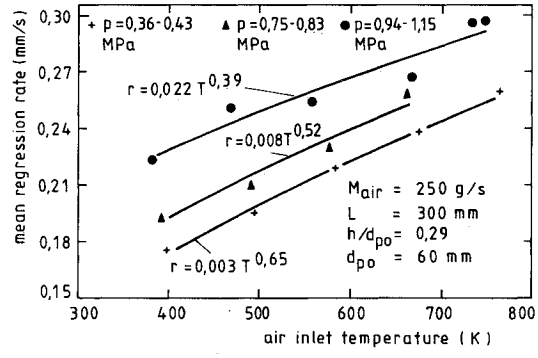

Fig. 10 Effect of inlet air temperature on regression rate.

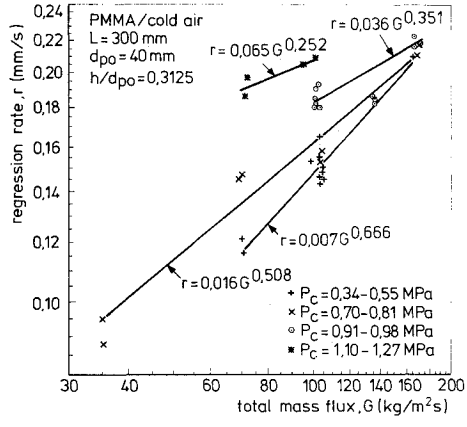

Fig. 8 Effect of mass flux on regression rate.

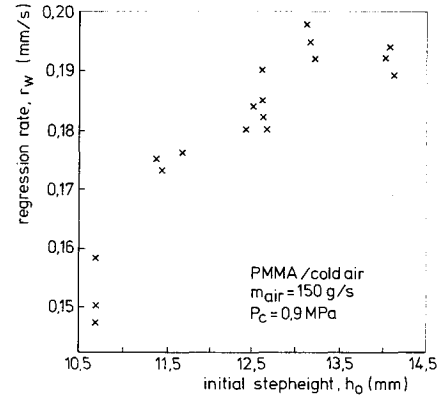

Fig. 11 Effect of stepheight on regression rate.

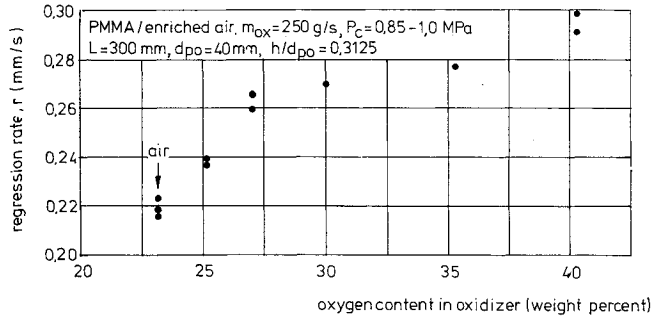

Fig. 9 Effect of oxygen content on regression rate.

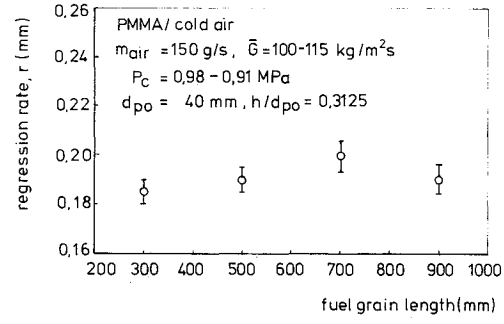

Fig. 12 Effect of grain length on regression rate.

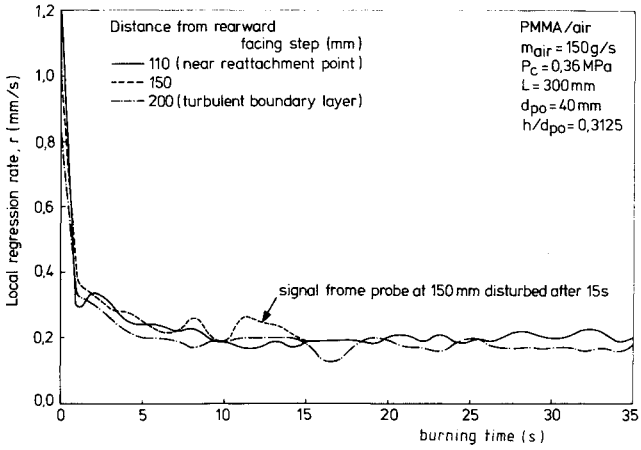

Fig. 13 Typical regression rate histories at three locations of the grain.

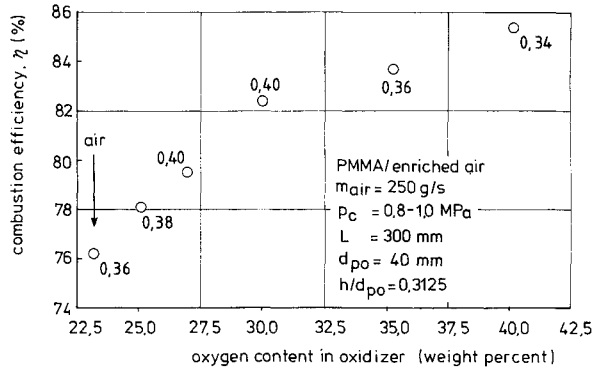

Fig. 14 Effect of oxygen content on combustion efficiency, the numbers near the data points indicate equivalence ratios.

At the three different locations, regression rate behavior is found to be roughly the same, which is in agreement with the observed flat inner profiles of the grain.

Combustion Efficiency

The combustion efficiency has been defined as the ratio between experimental and theoretical (according to chemical equilibrium) characteristic velocity. For mass flow rates between 100 and 250 g/s, and combustion pressures between 0.34 and 1 MPa, efficiencies range between 70 and 76%. An increase of the oxygen content in the air from 23 to 40 weight % increases the combustion efficiency from 76 to 86% (see Fig. 14).

The effect of the recirculation zone length L_r on combustion efficiency was investigated by varying the stepheight at constant grain length and by varying the grain length at constant stepheight (see Fig. 15). The recirculation zone is a region where, as indicated by the low temperatures measured, little reaction between fuel and oxidizer takes place. Downstream of this zone, mixing and combustion are more complete leading to increased efficiencies with increased ratios of L_g and L_r.

Detection of Radicals

Spectroscopic measurements during the combustion of PMMA, $(C_5\ H_8\ O_2)_n$, revealed spectra of the radicals CH, C_2, and OH (see Fig. 16). While OH and CH are often referred to in reaction kinetics modeling, C_2 usually is omitted. Nevertheless, during the experiments it appeared that the concentration of C_2 was comparable to that of CH.

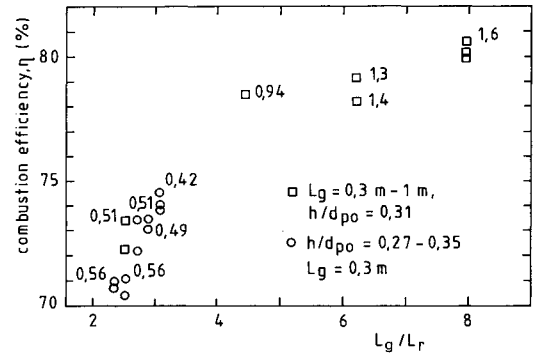

Fig. 15 Combustion efficiency vs L_g/L_r, the equivalence ratios are given next to the data points.

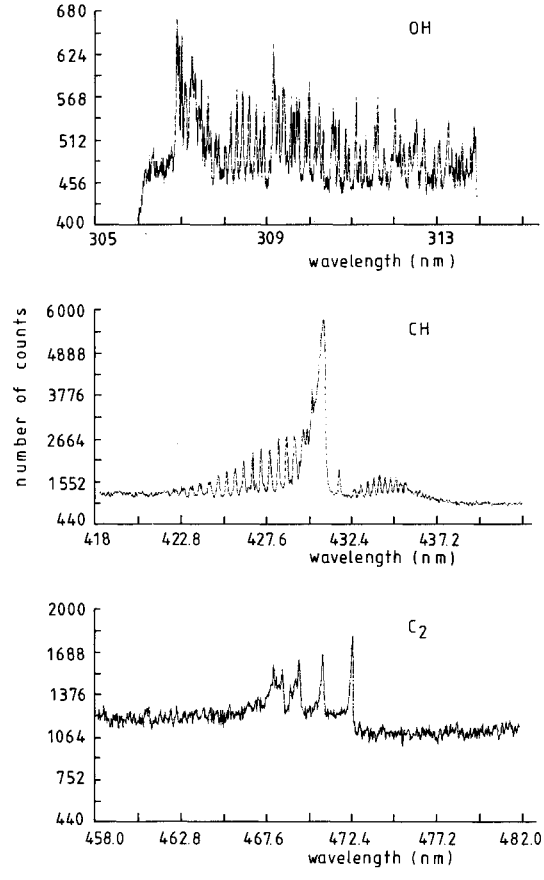

Fig. 16 Spectra of OH, CH, and C_2 observed with ambient air.

After ignition, the intensity of the OH-spectrum dropped by a factor of approximately 30 during the first 5 s, after which it remained constant. This reduction is attributed to the disappearance of the H_2/O_2 ignition flame.

Spectroscopically Determined Temperatures

Spectra of radiation from soot were analyzed. The variation in the soot absorption coefficient may be neglected in the wavelength region between 375 and 385 nm covered by the multichannel detector in the spectrograph. Hence the spectrum of the radiating soot can be considered to be one of a grey body with the same temperature.

From a calibrated tungsten ribbon lamp, reference spectra in the above mentioned wavelength region were recorded at temperatures between 1300 and 3000 K at 100 K intervals. In

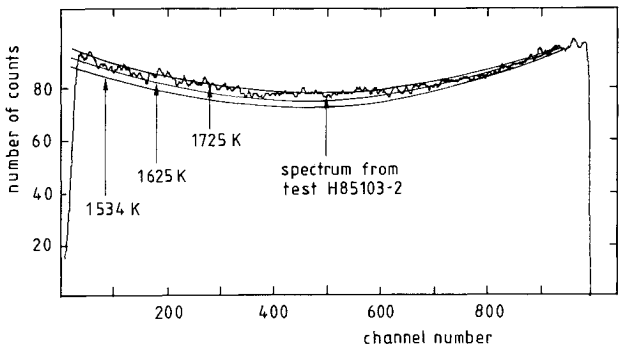

Fig. 17 Temperature using reference spectra obtained from "black-body" emitters.

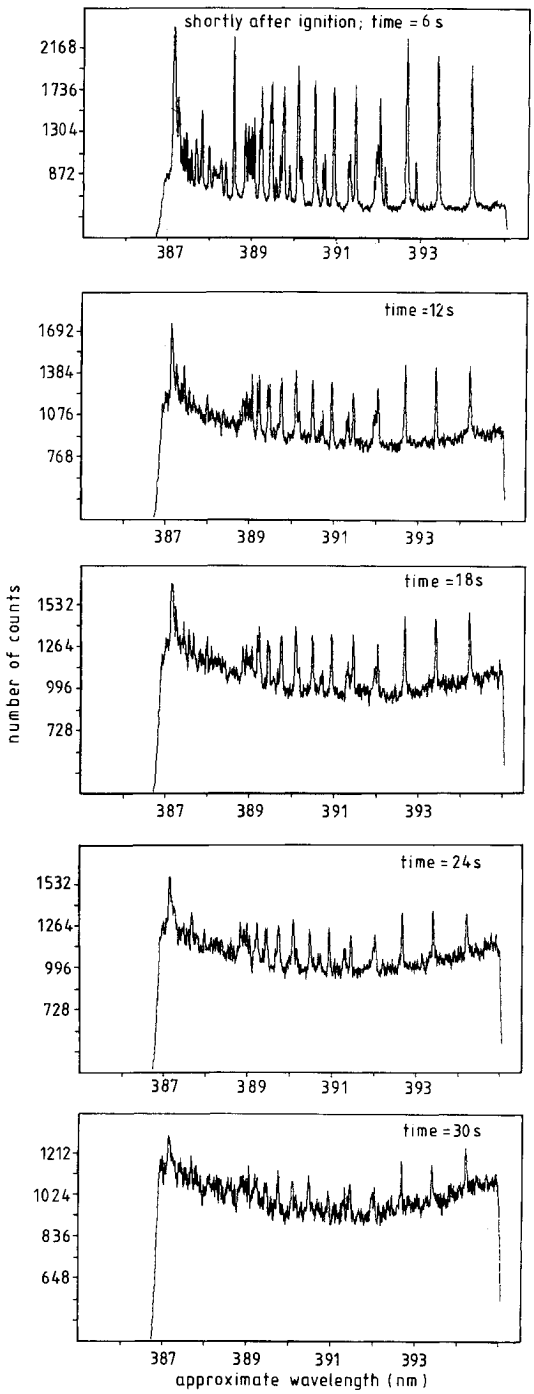

Fig. 18 Successive spectra of CH and soot at 390 nm (not processed, chamber pressure is 0.53 MPa).

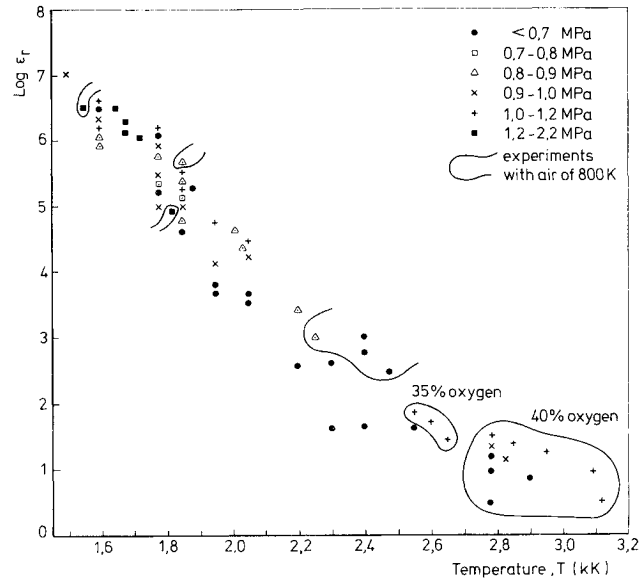

Fig. 19 Relative soot emissivity of soot ($\lambda = 380$ nm) vs temperature, pressure, inlet air temperature, and oxygen concentration.

the wavelength region used, tungsten can be considered as a grey body at these temperatures.[13] The measurements were made through a PMMA window, similar to the grain wall, and through a quartz window for comparison with axial observations. Soot radiation spectra from the combustion chamber have been compared with the above mentioned reference spectra of known temperatures. The flame temperature, which almost equals the soot temperature, is the temperature assigned to that reference spectrum that fits best (see Fig. 17). At the temperatures derived, and at 380 nm, the radiation intensity is calculated to be proportional to T_r^{20}; therefore, only maximum temperatures along the chordal beam were measured.

Figure 18 shows successive spectra of CH and soot taken 225 mm from the inlet at a mean pressure of 0.53 MPa. This figure again exhibits the relatively long time required to obtain full flame development already mentioned in relation to Fig. 4. Table 1 presents temperatures measured during experiments with cold air, heated air, and oxygen-enriched cold air.

During each test run usually 32 flame spectra were recorded successively at intervals of about 1 s. Data transfer required 33 ms after each exposure of 1 s.

According to the soot radiation spectra, some temperatures could only be estimated to be in the range 3000–5000 K. Another indication of such high temperatures is the increased relative intensity of the high-numbered rotational lines of CH with respect to the relative intensity of the same lines in a 2050 K butane flame.

From Table 1, two major effects are observed. First, below 0.6 MPa, the temperatures are significantly higher than at higher pressures. At low pressures, the variation in temperature during one experiment is considerably larger than at high pressures. Second, at higher pressures, experiments carried out with cold air (see Table 1a) have a tendency to level off at temperatures between 1600 and 1800 K; experiments with heated air (see Table 1b) show the same tendency. For oxygen-enriched air (see Table 1c), the combustion temperatures seem to be higher.

From visual observation of the burning fuel grain, it is noted that hardly any soot is present at low pressure. At higher pressures, soot is formed, and its concentration increases with pressure. As a result, radiation will also enhance regression rate.

In the wavelength region chosen, only soot contributes to the emissivity. Low emissivities are directly proportional to

Table 1a Results of spectroscopic measurements from PMMA combustion experiments with cold air; temperature accuracy 50 K unless specified otherwise

Distance from entrance, mm	p_c, MPa	m_a, g/s	Temperature, K Time after ignition, s 6	12	18	24	30	Remarks
75	0.92	262	2300	2300	2050	2050	1950	In recirculation zone
110	0.84	150	2050	1850	1600	1750	1750	
110	0.88	150	1750	1750	1600	——	——	Near reattachment point
110	0.90	150	1850	1850	1750	1750	1750	
110	0.92	150	1600	1600	1500	1600	1600	
225	0.35	149	[a]	[a]	2800	2800	2800	[b]
225	0.55	150	2550	2300	2050	2050	1950	[c]
225	0.78	96	1950	1850	1850	1750	1600	
225	0.80	149	1850	1600	1600	1600	1750	Developing boundary layer
225	0.80	150	1870	1660	1680	1720	1680	[d]
225	0.91	201	2050	1950	1850	1750	1750	
225	0.93	150	1750	1850	1850	1750	1850	
Axial	0.34	150	[a]	[a]	[a]	[a]	[e]	
Axial	0.53	149	2800	2400	2200	1950	1950	[f]
Axial	0.71	149	2050	2050	1750	1600	1750	
Axial	0.82	149	1750	1600	1600	1750	——	

[a]Temperature between 3000 and 5000 K. [b]100 K accuracy, decreasing line intensity. [c]Line intensity decreases to zero at increasing pressure. [d]Accuracy 30 K. [e]Irregular decreasing line intensity. [f]100 K accuracy, weak line intensity decreasing to zero at increasing pressure.

Table 1b Results of spectroscopic measurements from PMMA combustion experiments with air of 800 K; temperature accuracy 50 K unless specified otherwise

Distance from entrance, mm	p_c, MPa	m_a, g/s	Temperature, K Time after ignition, s 6	12	18	24	30	Remarks
150	0.40	146	——	3600[a]	2400	——	2400	Developing boundary layer
150	0.81	148	2250	2040	2010	1740	1850	[b]
150	1.49	149	——	1820	——	1550	——	[c]

[a]Accuracy 300 K. [b]Accuracy 30 K. [c]Accuracy of 100 K.

Table 1c Results of spectroscopic measurements from PMMA combustion experiments with oxygen-enriched air; temperature accuracy 50 K unless specified otherwise

Distance from entrance, mm	p_c, MPa	m_a, g/s	Oxygen content weight %	Temperature, K Time after ignition, s 6	12	18	24	30	Remarks
225	0.85	254	25	2050	2050[a]	——	——	——	
225	0.85	253	25	2900[a]	2050	2050	——	——	
225	0.90	252	27	2900[a]	2650[a]	2400	2400	2300	Developing boundary layer
225	0.96	246	35	——	——	2550	2600	2660	[b]
225	0.97	248	40	2910	2780	2780	2780	3110	[b]
225	1.00	256	40	2780	2820	3090	2950	2850	[b]

[a]Accuracy 100 K. [b]Accuracy 30 K.

the soot concentration. Relative emissivities were obtained from the ratio between measured spectral intensities and calculated ones of blackbody radiators at the determined temperatures. The results are shown in Fig. 19 for cold air, air at 800 K, and oxygen-enriched cold air. Based on the intensities of the reference spectra, it is estimated that an emissivity of unity occurs at about 1700 K. The data in Fig. 19 suggest an even higher emissivity at lower temperatures, which indicates rather large measurement errors. Nevertheless, some interesting conclusions are drawn from this figure.

There is good agreement between the results for cold air and air at 800 K: the emissivity decreases with temperature and increases with pressure. For the experiments with oxygen-enriched air, the emissivity is remarkably lower, even at high pressure. It is concluded that oxygen enrichment favors good combustion. The observed emissivity-pressure dependency supports the assumption made earlier that the observed increase in regression rate with increasing pressure is caused by radiation from soot. After the gas/soot mixture has become optically dense, increase in soot concentration does not yield an increase in radiation, which explains the observed leveling off of the regression rate at higher pressures.

Conclusions

Combustion experiments with PMMA in a solid fuel ramjet showed that mass flux, pressure, oxygen content, and inlet air temperature directly affect the regression rate. Stepheight and fuel grain length are of secondary importance. The regression

rate increases with mass flux and inlet air temperature. At low pressures the regression rate is independent of pressure, but above a threshold it increases with pressure to reach a limiting value, because of the formation of soot. Soot generation is suppressed by increasing the oxygen content in the air. The experiments took place at relatively small mass fluxes. The radiative heat transfer appeared to be of the same order as the convective heat transfer and therefore could explain the observed increase in regression rate.

The highest temperatures occur at low pressures and hence at low soot concentrations. Although the occurrence of OH and CH was expected, the observation of a significant concentration of C_2 may imply that combustion modeling for PMMA has to be adjusted.

Acknowledgments

This work has been supported by the Technology Foundation (STW) and the Project Management Office for Energy Research (PEO) in the Netherlands.

References

[1]Korting, P. A. O. G., and Schöyer, H. F. R., "Experimental Connected Pipe Facility for Solid Fuel Ramjet Combustion Studies," *Proceedings of the Internationale Jahrestagung* ICT 1984, Karlsruhe, 1984.

[2]Wijchers, T., "A Method for Spectroscopic Temperature Measurements in a Solid Fuel Combustion Chamber," Delft University of Technology/Prins Maurits Laboratory TNO, Rijswijk, The Netherlands, Memorandum M-530/Rept. PML 1985-C7, 1985.

[3]Elands, P. J. H., and Wijchers, T., "Visible Radiation Measurement for Temperature Determination," Delft University of Technology/Prins Maurits Laboratory TNO, Rijswijk, The Netherlands, Rept. LR-479/PML 1985-C74, 1985.

[4]Korting, P. A. O. G., and Schöyer, H. F. R., "Determination of the Regression Rate in Solid Fuel Ramjets by Means of the Ultrasonic Pulse Echo Method," *Heat Transfer in Fire and Combustion Systems,* American Society of Mechanical Engineers, New York, HTD-Vol. 45, 1985.

[5]Vos, J. B., "The Calculation of Turbulent Reacting Flows with a Combustion Model Based on Finite Chemical Kinetics," Ph.D. Thesis, Delft University of Technology, Delft, The Netherlands, 1987.

[6]van der Geld, C. W. M., "On the Direct Simulation of Vortex Shedding," Delft University of Technology, Delft, The Netherlands, Rept. LR-513, SFCC-publication 40/Rept. PML 1987-C17, 1987.

[7]Mady, C. J., Hickey, P. J., and Netzer, D. W., "Combustion Behaviour of Solid-Fuel Ramjets," *Journal of Spacecraft and Rockets,* Vol. 15, May-June 1978, pp. 131–132.

[8]Muzzy, R. J., "Applied Hybrid Combustion Theory," AIAA Paper 72-1143, 1972.

[9]Kops, J. J. T., "Een model voor de Verbranding van Poly Methyl Methacrylaat in Lucht in een Laminaire Diffusie Vlam," Delft University of Technology/Prins Maurits Laboratory TNO, Rijswijk, The Netherlands, Rept. LR-439/PML 1984-C75, 1984.

[10]Metochianokis, M. E., and Netzer, D. W., "Modeling Solid-Fuel Ramjet Combustion, Including Radiation to the Fuel Surface," *Journal of Spacecraft and Rockets,* Vol. 20, April 1983, pp. 405–406.

[11]Elands, P. J. M., Korting, P. A. O. G., Dijkstra, F., and Wijchers, T., "Combustion of Polyethylene in a Solid Fuel Ramjet—A Comparison of Computational and Experimental Results," AIAA Paper 88-3043, July 1988.

[12]Zvuloni, R., Levy, Y., and Gany, A., "Experimental Investigation of a Solid Fuel Ramjet Combustor," *Proceedings of the 28th Israel Annual Conference on Aeronautics and Astronautics,* Kenes, Tel Aviv, Israel, 1986.

[13]de Vos, J. C., "The Emissivity of Tungsten Ribbon," Ph.D. Thesis, Vrije Universiteit, Amsterdam, 1953 (Dutch).